

## Supporting Information

### Near infrared spectra of high-density crystalline H<sub>2</sub>O ices II, IV, V, VI, IX & XII

Christina M. Tonauer<sup>1</sup>, Eva-Maria Köck<sup>1,3</sup>, Tobias M. Gasser<sup>1</sup>, Violeta Fuentes-Landete<sup>1,3</sup>,  
Raphael Henn<sup>2</sup>, Sophia Mayr<sup>2</sup>, Christian G. Kirchler<sup>2</sup>, Christian W. Huck<sup>2</sup> & Thomas  
Loerting<sup>\*,1</sup>

<sup>1</sup> Institute of Physical Chemistry, University of Innsbruck, A-6020 Innsbruck, Austria

<sup>2</sup> Institute of Analytical Chemistry and Radiochemistry, University of Innsbruck, A-6020  
Innsbruck, Austria

<sup>3</sup> Max-Planck-Institut für Chemische Energiekonversion, D-45470 Mülheim an der Ruhr,  
Germany.

e-mail: [thomas.loerting@uibk.ac.at](mailto:thomas.loerting@uibk.ac.at)

**Figure S1:** Powder X-ray diffractograms (XRD) of all high-pressure ice samples using Cu  $K_{\alpha 1}$  radiation (wavelength: 1.5406 Å). Each pattern represents a single scan of a given ice polymorph, so that each panel allows to judge on reproducibility. Reference diffractograms (bottom row of each panel) are calculated from published neutron or X-ray data for ices II (ref. 30), IV (ref. 31), V (ref. 32), VI (ref. 33), IX (ref. 34) and XII (ref. 35) using crystallography data analysis software GSAS-II. Slight shifts of Bragg peaks compared to literature data stem from different T-p conditions. While diffractograms shown in this study were measured at 77 K and subambient pressure ( $\sim 10$  Pa), the literature data were collected at different conditions (ice II: 110 K/ambient pressure, ice IV: 210 K/0.7 GPa, ice V: 98 K/ambient pressure, ice VI: 225 K/1.1 GPa, ice IX: 110 K/ambient pressure, ice XII: 260 K/0.5 GPa). Signals resulting from the Cu and Cu/Ni sample holders are marked with vertical lines and asterisks. The ice IV samples contain minor amounts of ice XII since both reaction channels, the formation of ice IV and the formation of ice XII, are operative upon heating uHDA at 0.8 GPa <sup>36</sup>.

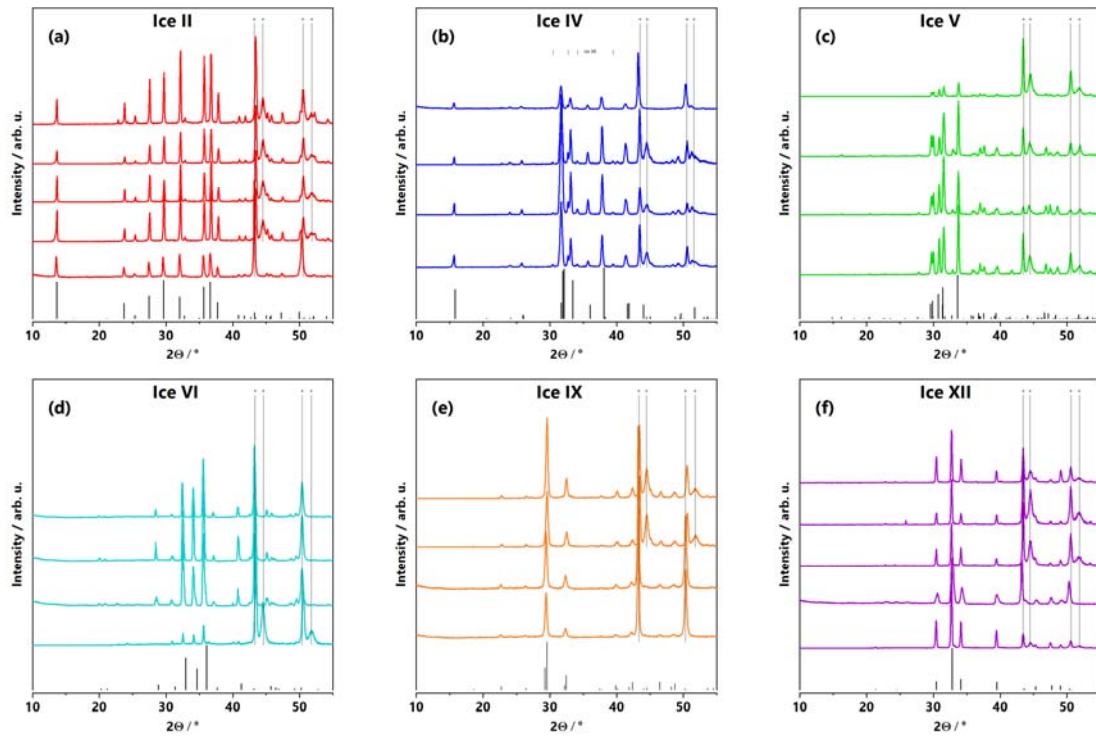


**Figure S2:** Optical microscope image of a powdered ice sample (ice I<sub>h</sub>) at 248 K. The photograph shows the typical size range of grains in powdered ice samples used in the present NIR study (15 to 40 μm for single grains and up to 350 μm for larger grain aggregates).

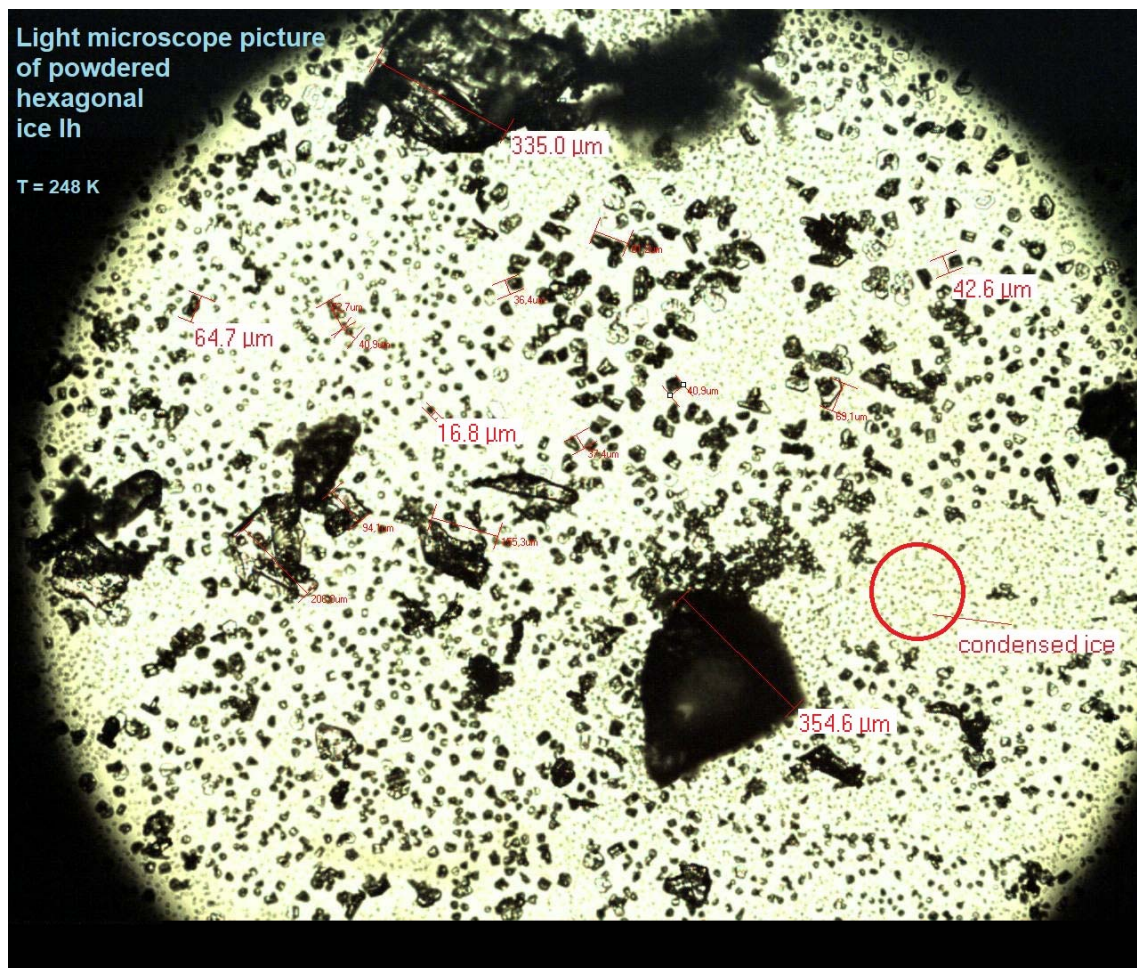


**Fig. S3:** Depiction of the baseline correction procedure used in the present study for all raw spectra. A basis spline function was constructed from 8 anchor points (purple circles) and then subtracted from the raw spectrum.

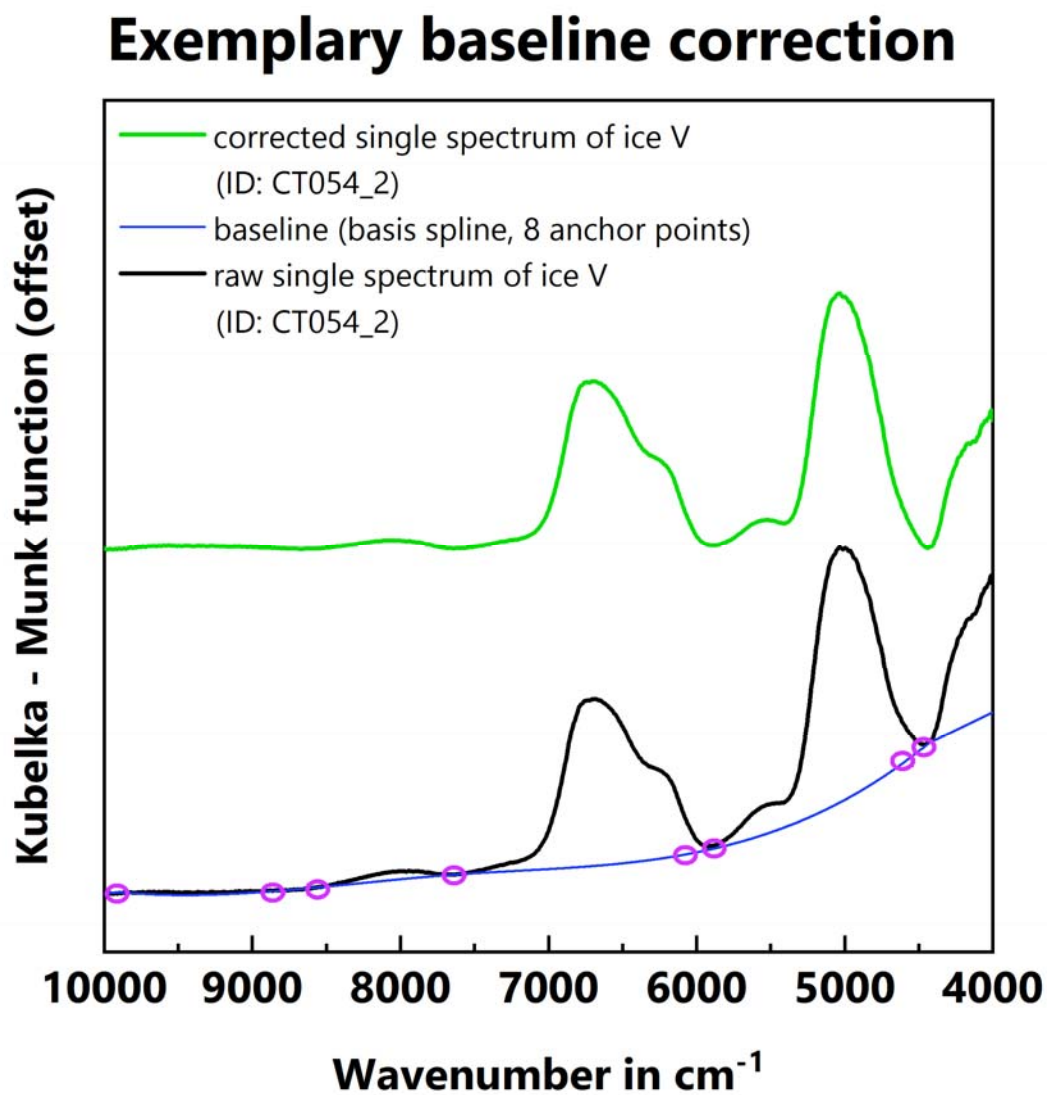


**Fig. S4:** Identification of peak centres and shoulders using first and second derivative spectra of the K-M function spectra (shown for ice V): For locating the peak centre of the K-M function the zero crossings of the first derivative were considered. Shoulders were identified through minima in the first derivative and zero crossings in the second derivative spectrum.

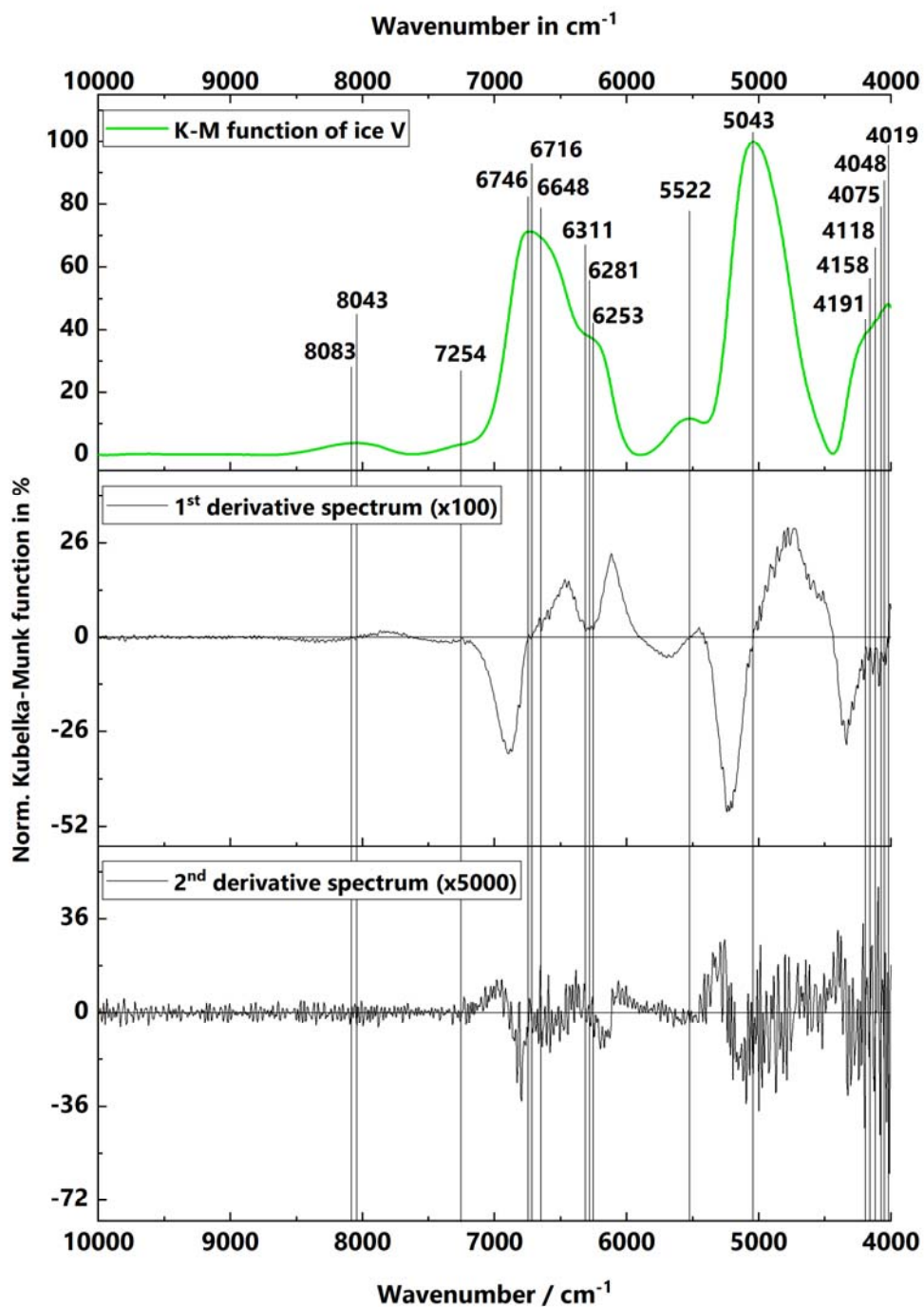


Table S1: Normalized Kubelka-Munk function in % for ices I<sub>h</sub>, II, IV, V, VI, IX and XII shown in Fig 1 and Fig 2(ab)

File name: S Table 1.txt

Tables S2-S8: Raw Kubelka-Munk function spectra for ices I<sub>h</sub>, II, IV, V, VI, IX and XII

File names: S Table 2\_I<sub>h</sub> raw.txt

S Table 3\_II raw.txt

S Table 4\_IX raw.txt

S Table 5\_IV raw.txt

S Table 6\_V raw.txt

S Table 7\_VI raw.txt

S Table 8\_XII raw.txt